# Predicting the performance of an epilimnetic bubble-plume mixer in a shallow reservoir using a three-dimensional hydrodynamic model

Shengyang Chen [1, a*], Chengwang Lei [1, b], Cayelan C. Carey [2, c], and John C. Little [3, d]

[1] School of Civil Engineering, The University of Sydney, Sydney, NSW 2006, Australia
[2] Department of Biological Sciences, Virginia Tech, Blacksburg, VA 24061, USA
[3] Department of Civil and Environmental Engineering, Virginia Tech, Blacksburg, VA 24061, USA

[a] shengyang.chen@sydney.edu.au, [b] chengwang.lei@sydney.edu.au, [c] cayelan@vt.edu, [d] jcl@vt.edu

**Keywords:** Mixing, Bubble plume, Hydrodynamic model, Destratification, Water quality

**Abstract.** Artificial mixing with bubble-plume devices is often used to deal with water quality problems in reservoirs, such as algal bloom and hypoxia. In general, the mixing results in an increase of dissolved oxygen in the water, as well as an increase in temperature in the deeper layers of the water body but a decrease in temperature in the upper layers. Understanding the heat and oxygen transfer mechanisms will help to optimise the design and operation of the devices.

This study focuses on Falling Creek Reservoir (FCR), which is a shallow, eutrophic drinking water reservoir managed by the Western Virginia Water Authority, Virginia, USA. FCR is equipped with a bubble-plume epilimnetic mixer (EM) to cope with occasional algal blooms during the stratified periods. We adopt a validated three-dimensional hydrodynamic model Si3D to visualise and analyse the mixing performance of the EM in FCR. It is found that the mixing with the EM placed in the deep region of FCR has a significant impact on the water temperature throughout the reservoir. The mixing reduces thermal stability, increases the metalimnetic temperature, and deepens the thermocline. Tracers are used in the model to further quantify the mixing performance of the EM.

## Introduction

Various mixing and oxygenation systems are used to control water quality problems such as algal bloom and hypoxia. Common oxygenation and mixing systems include bubble-plumes [1], airlift aerators [2], Speece cones [3], and side-stream oxygenation systems [4, 5]. Among these systems, bubble-plume systems have been widely used to add oxygen and mix lakes and reservoirs (e.g. [6, 7]). However, the mixing outcomes have not always been consistent. Although McGinnis et al. [8] showed that the bubble-plume devices can successfully add oxygen to water and mitigate water quality problems, Nurnberg et al. [9] showed that improper mixing increased phosphorous transfer from the hypolimnion to the epilimnion, thereby causing surface algal blooms. Therefore, understanding the heat and oxygen transfer mechanisms is of importance when the bubble-plume systems are designed for water management.

In the present study, Si3D, a three-dimensional hydrodynamic model, is employed to analyse a bubble-plume epilimnetic mixing (EM) system. The effect of mixing on the thermal structure and substance transport is of interest.

## Methodology

The numerical model is built based on the bathymetric information collected from Falling Creek Reservoir (FCR), as shown in Figure 1a. Apart from the Si3D hydrodynamic model which is described in [10], a coupled bubble-plume model will be adopted to simulate the flow induced by the EM system which is placed 5 m below the water surface at a location by the white lines in Figure 1a. The theory behind the bubble-plume model is well established (e.g. [7, 11]). A schematic representation of the model is provided in Figure 1b.

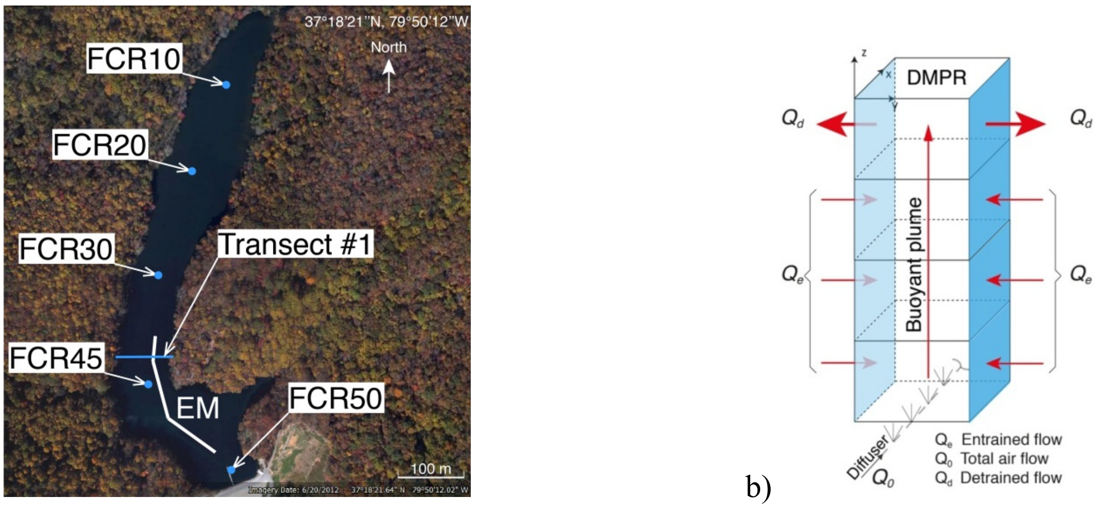


a) b)

**Figure 1. a) Schematic diagram of sampling locations. The corresponding locations are sampled in the numerical model. b) Schematic diagram of the bubble plume model with grid cells. The grid cells serve as sinks and relocate the entrained water from the lower to the upper grid cell. The top grid cell is at the Depth of Maximum Plume Rise (DMPR), serving as a source to discharge or detrain the plume water.**

The meteorological data from a single day in 2015 near FCR are repeated for the entire simulated period. The schedule for the EM operation in the numerical model is shown in Table 1.

**Table 1. Numerical operation scheme for EM**

| Days | 1 | 2 – 8 |
|---|---|---|
| EM | OFF | ON |

## Results

The effect of EM mixing on the thermal structure and substance transport in the water body is the focus of this investigation. The three-dimensional behaviour of mixing is visualised using the contours of temperature and tracers.

**Effect of Mixing on the Temperature Structure.** With the continuous operation of EM, the overall water temperature in the metalimnion increases as seen in Figure 2, which shows that the effect of mixing is significant. In order to quantify the variation of the thermal structure as the result of mixing, the concept of Schmidt stability, which characterizes the resistance to mechanical mixing due to potential energy inherent in the stratified water as reported in [12], is adopted. The time series of the calculated Schmidt stability is plotted in Figure 2 (the white dash-dotted curve). It can be seen in Figure 2 that EM mixing reduces the thermal stability in the water column.

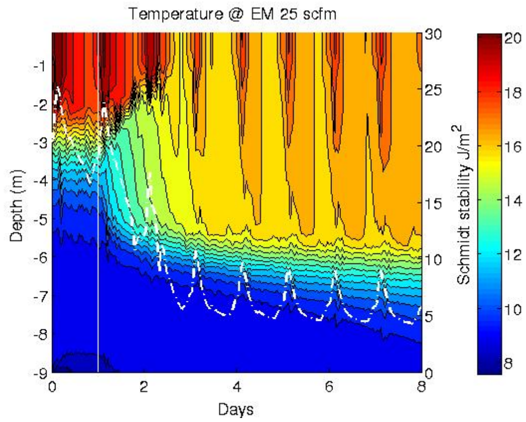


**Figure 2. Temperature contour and Schmidt Stability. The white dashed curve over the contour indicates the Schmidt stability variation as a function of time. The white vertical line indicates when the EM system is activated.**

Figure 3 shows the instantaneous temperature structures under the effect of EM mixing at different time instants. The observation in Figure 3 suggests that the surface water temperature decreases due to the operation of the EM system while the thermocline is deepened. The water temperature near the thermocline is homogenised as a result of mixing. It is interesting to see that the influence of mixing is not limited to the surrounding area of the EM diffuser; the mixing also affects the water in the region far beyond the diffuser line. A similar trend can be observed beyond the diffuser line between the sampling sites FCR20 and FCR30. However, the site FCR10 is too shallow and too far to be affected by the EM mixing.

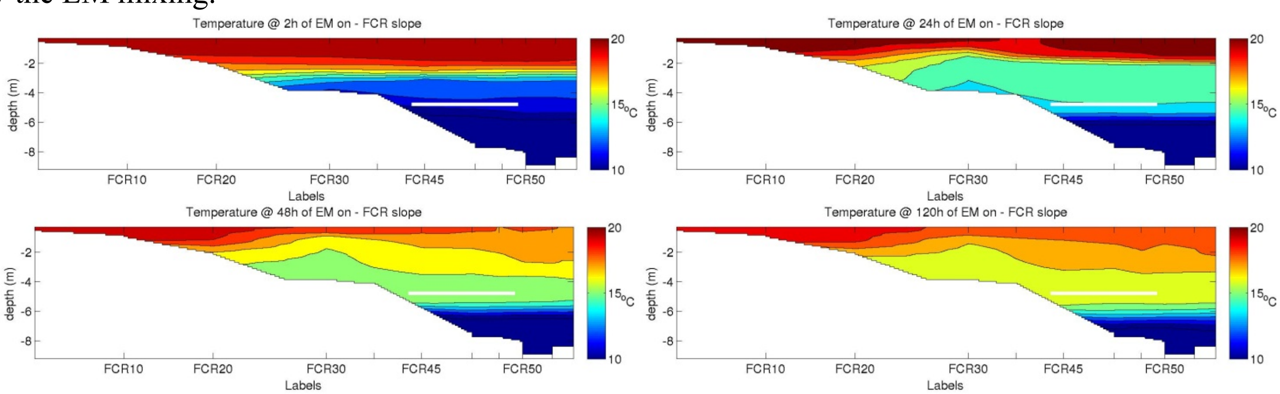


**Figure 3 Instantaneous temperature structures across the reservoir with EM at 25-scfm flow rate. The white horizontal lines indicate the approximate location and depth of the EM diffuser.**

**Effect of Mixing on Substance Transport.** In order to quantify the substance transport induced by the EM system, tracers are added into the water along with the flow from the EM system. The tracers are passive non-reactive scalars in the model.

The contours of model-predicted tracer concentrations over time for two different flow rates (15 and 25 scfm) are shown in Figure 4. The temporal development of the tracer distribution in FCR50 shown in this figure may indicate the influence of mixing on substance transport. As shown in Figure 4b, the detrained plume is evenly spreading out at the DMPR. The vertical extent of the region affected by the EM operation (i.e. the region with tracers shown in Figure 4) expands with time, which may be characterised by a parabolic function of time, as indicated by the white curves in the figure. This trend continues until the tracers reach the surface mixing layer, where intensive convective mixing takes place due to the turbulence generated by wind and surface heat fluxes.

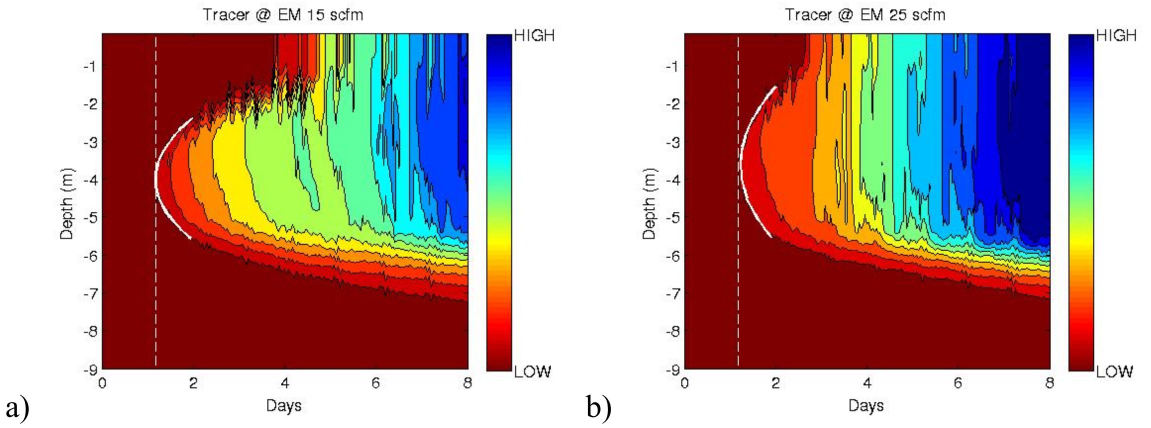


**Figure 4 Time series of tracer concentration development at FCR50. The contour bars show the colour scheme for tracer concentration (from zero). The white vertical dashed lines indicate when the EM system is activated.**

The parabolic function shown in Figure 4 is given by:

$$x = a(y - h_{top})^2 \quad (1)$$

where $h_{top}$ is the DMPR, $x$ represents the duration of the EM system in operation (days), $y$ represents the depth that the tracers can reach (m), and $a$ is an indicator of the resistance to substance transport in water. With the higher mixing energy of the EM system (i.e. with the higher EM flow rate), the resistance is lower because of the fact that EM mixing enhances substance transport in water. Therefore, the parabolic function given in Equation (1) may be used to quantify the strength of the vertical mixing induced by the EM operation.

**Table 2 Mixing characteristics with EM flow rates**

| EM flow rate Q (scfm) | 10 | 15 | 20 | 25 | 30 |
|---|---|---|---|---|---|
| $a$ | 0.436 | 0.315 | 0.234 | 0.182 | 0.134 |
| $t_s$ (Days) | 4.130 | 2.573 | 1.595 | 1.455 | 1.092 |

In this study, the effect of the EM operation on substance transport is investigated at five different flow rates, as shown in Table 2. The above parabolic function is applied to the boundary of the mixing region to obtain the resistance indicator a, which is given in Table 2 for the different flow rates. It is found that the resistance indictor $a$ correlates well with the EM flow rate $Q$, as shown in Figure 5a. The correlation is given as follows:

$$\mathrm{a} = 0.785 * \mathrm{e}^{-0.060\mathrm{Q}} \quad (2)$$

Clearly, the time required for tracers to reach the surface ($t_s$) also depend on the EM flow rate (Table 2). The time $t_s$ may indicate the efficiency of mixing and is characterised by the time instant corresponding to mixing boundary reaching the water surface, which is measured on the contour where the tracer concentration near the surface becomes greater than zero. With a higher flow rate, the mixing time is shorter. Figure 5b shows the correlation between the time $t_s$ and the flow rate $Q$ with an exponential fitting curve. The expression is given as follows:

$$\mathrm{t_s} = 8.564 * \mathrm{e}^{-0.0762\mathrm{Q}} \quad (3)$$

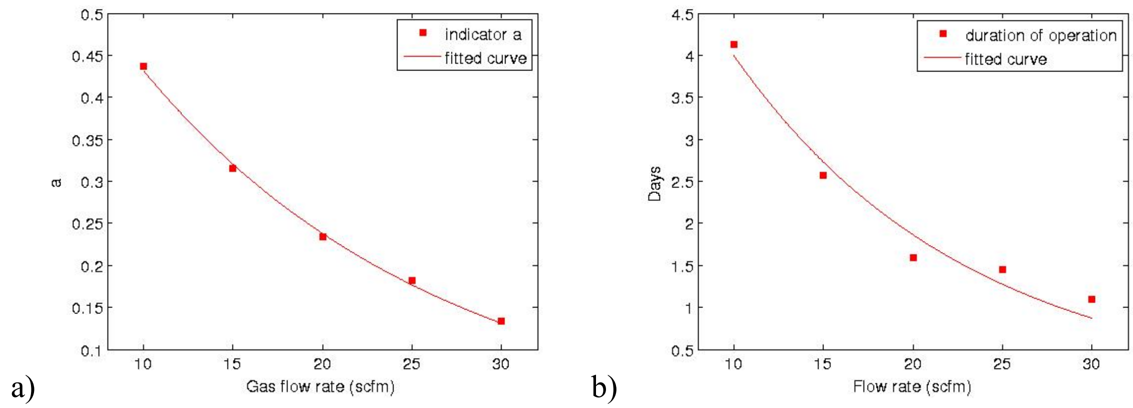


**Figure 5 Correlation between: a) EM flow rate and the resistance indicator a, b) EM flow rate and the time for tracers to reach the water surface.**

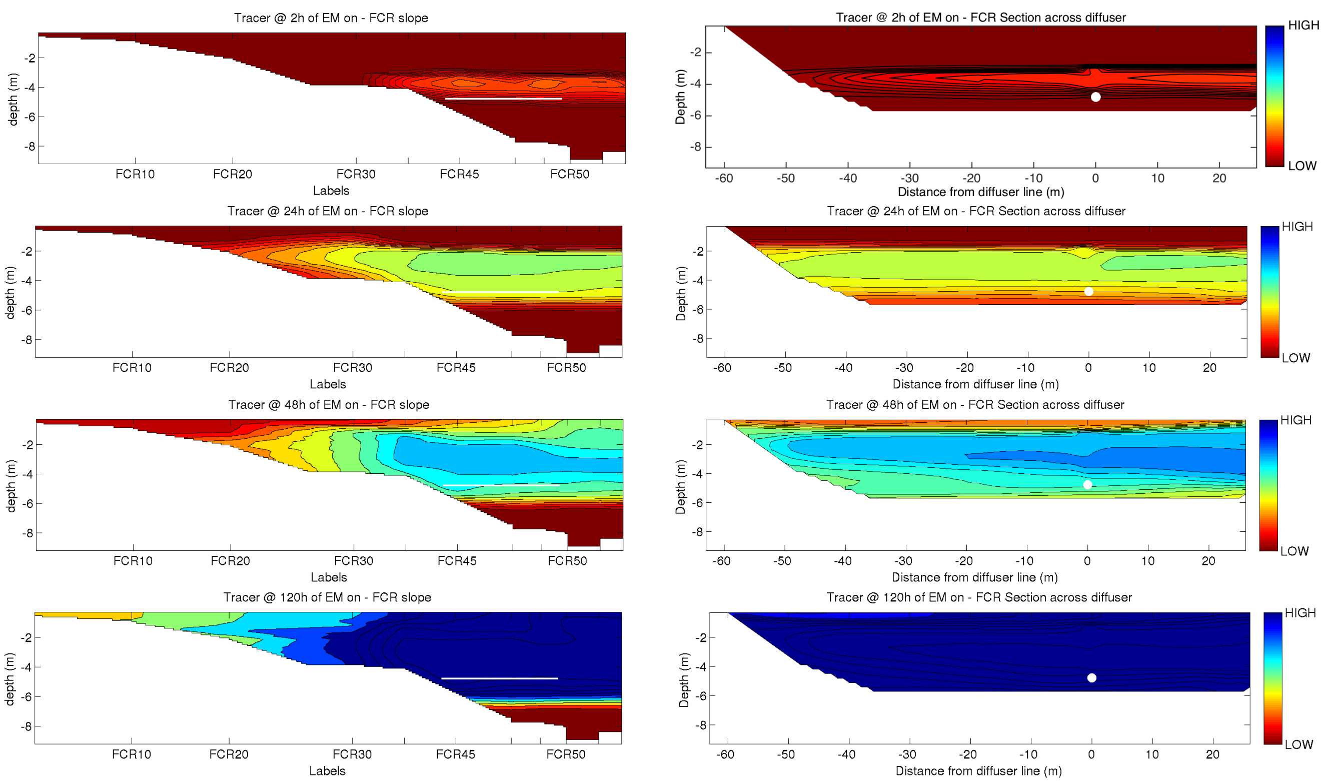


**Figure 6 Instantaneous response of the tracer concentration at 25 scfm. The contour bars show the colour scheme for tracer concentration. The white lines and dots in the figures indicate the location of the EM diffuser line. The figures on the right are collected from Transect #1 as shown in Figure 1a.**

The longitudinal extent of the region affected by the EM operation is shown by the instantaneous tracer concentration contours in Figure 6. With continuous running of EM for several days, tracers can reach most regions of FCR. It is seen in Figure 6 that the EM successfully mixed the entire water column above the diffuser. It is also seen in Figure 6 that tracers do not reach the hypolimnion in the bottom of the deep region of FCR (near FCR50). This is due to the weak circulation below the EM diffuser line, leaving the deeper layers at FCR50 undisturbed.

## Conclusion

The study has examined the effect of mixing by the EM system using a 3D hydrodynamic model Si3D coupled with a bubble-plume model. The results show that mixing with the EM placed in the deep region of FCR has a significant impact on the water temperature across the reservoir. The mixing reduces thermal stability, increases the metalimnetic temperature, deepens the thermocline, and enhances substance transport within the reservoir. It is found that the EM is a valuable tool for water management in terms of water temperature manipulation and substance transport.

## Acknowledgements

This research is supported by The University of Sydney in Australia, and Virginia Tech and Western Virginia Water Authority in USA.

## References

1. V.L. Singleton, P. Gantzer, J.C. Little, Linear bubble plume model for hypolimnetic oxygenation: Full-scale validation and sensitivity analysis, Water Resources Research, 43 (2007).
2. V.L. Burris, D.F. McGinnis, J.C. Little, Predicting oxygen transfer and water flow rate in airlift aerators, Water Research, 36 (2002), 4605-4615.
3. D.F. McGinnis, J.C. Little, Bubble dynamics and oxygen transfer in a speece cone, Water Science and Technology, 37 (1998), 285-292.
4. A.W. Fast, W.J. Overholtz, R.A. Tubb, Hypolimnetic oxygenation using liquid oxygen, Water Resources Research, 11 (1975), 294-299.
5. A.B. Gerling, R.G. Browne, P.A. Gantzer, M.H. Mobley, J.C. Little, C.C. Carey, First report of the successful operation of a side stream supersaturation hypolimnetic oxygenation system in a eutrophic, shallow reservoir, Water Research, 67 (2014), 129-143.
6. S.G. Schladow, Lake Destratification by Bubble-Plume Systems: Design Methodology, Journal of Hydraulic Engineering, 119 (1993), 350-368.
7. V.L. Singleton, J.C. Little, Designing hypolimnetic aeration and oxygenation systems - A review, Environmental Science and Technology, 40 (2006), 7512-7520.
8. D.F. McGinnis, A. Lorke, A. Wüest, A. Stöckli, J.C. Little, Interaction between a bubble plume and the near field in a stratified lake, Water Resources Research, 40 (2004).
9. G.K. Nürnberg, B.D. LaZerte, D.D. Olding, An Artificially Induced Planktothrix rubescens Surface Bloom in a Small Kettle Lake in Southern Ontario Compared to Blooms World-wide, Lake and Reservoir Management, 19 (2003), 307-322.
10. P.E. Smith A semi-Implicit, three-dimensional model for estuarine circulation, (2006).
11. A. Wüest, N.H. Brooks, D.M. Imboden, Bubble plume modeling for lake restoration, Water Resources Research, 28 (1992), 3235-3250.
12. S.B. Idso, On the concept of lake stability, Limnology and oceanography, 18 (1973), 681-683.